ACS APPLIED ENERGY MATERIALS

www.acsaem.org
Article

Improving the Volumetric Capacity of Gallocyanine Flow Battery by Adding a Molecular Spectator

Eduardo Martínez-González* and Pekka Peljo*

Cite This: https://doi.org/10.1021/acsaem.4c00971
Read Online

ABSTRACT: Gallocyanine (**GAL**) was recently introduced as a promising aqueous-soluble electroactive molecule for preparing two-electron storage alkaline flow battery (FB) negolytes. The development of a cost-effective **GAL** FB electrolyte is limited by the unexpectedly low solubility of **GAL**. In this work, the compound 7-amino-4-hydroxy-2-naphthalenesulfonic acid was introduced as a molecular spectator to modulate the solubility of **GAL** in KOH; this formulation allowed the preparation of a negolyte with a theoretical volumetric capacity of 32.00 Ah L^{-1}. The cycling stability of an improved **GAL** electrolyte was demonstrated by operating a FB cell outside of the glovebox (bubbling N_2 in the tanks). The cell exhibited a Coulombic efficiency close to 98% and began operating with 72.1% of its theoretical capacity (16.06 Ah L^{-1}), retaining 88% of it after 110 cell cycles. This work demonstrates that significant improvement in electrolyte performance can be obtained with suitable additives and electrolyte engineering.

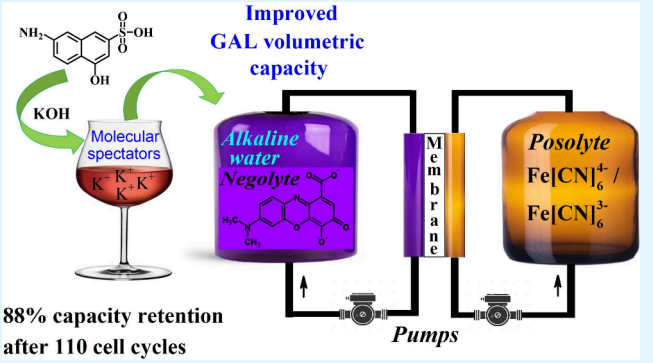

KEYWORDS: *Alkaline flow batteries, two-electron storage negolyte, additive, molecular spectator, improved gallocyanine solubility, ion pairing interactions*

1. INTRODUCTION

Flow batteries (FBs) are promising technologies for large-scale and mid-duration storage of renewable electricity.[1−4] This technology utilized electricity to charge posolyte (solution to store positive charge) and negolyte (solution to store negative charge) electrolytes inside an electrochemical cell, which are subsequently pumped into external tanks for storage. In this configuration, the power output and energy density are decoupled: the latter parameters can be modulated by changing the cell-stack and tank sizes, respectively.

Recently, aqueous organic FBs were introduced as a low-cost alternative to the present metal-based technology.[5,6] Organic batteries are assembled with abundant and less toxic electroactive-materials displaying tunable chemical (e.g., solubility) and electrochemical properties (e.g., redox potentials).[1] A wide variety of organic-electroactive compounds (some examples are quinones,[6] phenothiazines,[7] alloxazines,[8] and viologens[9]) have been proposed to prepare negolyte solutions, among which two-electron storage based-structures are crucial for doubling of charge storage capacity and increasing the energy density.[1,7−10] They can also enable the realization of long-lifetime FBs,[10] but these systems are scarce, since most compounds undergo irreversible two-electron reduction reactions in aqueous media.[1] Another promising approach is to improve the performance of the base structures that worked successfully.

The development of cost-effective FB negolytes requires achieving high volumetric capacity, which depends on the number of electrons stored per molecule and can be significantly improved by increasing the aqueous solubility of the electroactive species.[9,11,12] Solubility usually increases by incorporating the following ionic groups in the molecules:[1,11] $-SO_3^-$, $-O^-$, $-COO^-$, $-PO_3^{2-}$, $-NR_3^+$, but there are some cases where solubility does not improve significantly and the reason is not clearly understood.[1,13,14] Furthermore, synthetic routes to incorporate these solubilizing groups can be expensive and have low reaction yields.[4]

A promising group of air-stable electroactive materials to prepare aqueous FB electrolytes are phenothiazine and phenoxazine heteroaromatic compounds.[1,15,16] They exhibit a reversible two-electron transfer process and can be charged−discharged outside a glovebox, which is interesting because

Received: April 17, 2024
Revised: August 6, 2024
Accepted: August 9, 2024

most of the reported batteries in the literature were operated under inert atmospheres due to degradation and/or faradaic imbalance of the electrolytes caused by traces of oxygen infiltration.[17−19]

The long-term cycling stability of the former compounds working in a less-restricted atmosphere condition was proved in acidic solutions,[15,16] and also in alkaline electrolytes for the case of phenoxazine-based gallocyanine structure.[1] The latter system undergoes a single two-electron reduction process and is also relevant for medicine and other electronic applications.[20−23] This compound was chosen as a FB negolyte because it is one of the commercially available phenoxazines and its structure is decorated with OH and COOH groups that can be deprotonated to form water-soluble negatively charges species $\mathbf{GAL}_{ox}^{2-}$ (Scheme 1).[1]

Scheme 1. Chemical Structure of Gallocyanine Deprotonated Species ($\mathbf{GAL}_{ox}^{2-}$) and 7-Amino-4-hydroxy-2-naphthalenesulfonic Acid (AHSQ) Compounds Studied

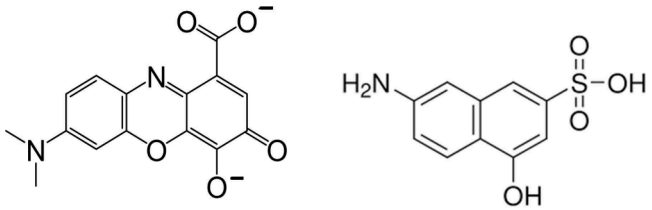

The **GAL**-KOH negolyte solution showed good cycling stability (during 200 charge−discharge cell cycles) when tested in a cell (bubbling N_2 into the tanks) outside the glovebox. However, the deprotonated species $\mathbf{GAL}_{ox}^{2-}$ was poorly soluble (<0.1 mol L^{-1}); so, the negolyte solution contained only 0.05 mol L^{-1} of active species. Therefore, it is promising to work on improving the volumetric capacity of **GAL**-KOH negolyte, for instance, by reformulating the electrolyte.[4]

It is well-known that additives such as urea can significantly decrease hydrophobic interactions, decreasing dimerization and increasing solubility,[24−27] and this was utilized to improve solubility of flow batteries.[28] As reported by Liu et al.,[29] the addition of molecular spectator α-cyclodextrin suppressed dimerization interactions in a methyl viologen FB electrolyte, improving its cycling lifetime. Likewise, ethylene glycol and tetramethylammonium cations prevented the decomposition mechanism[30] and improved the solubility[31] of quinone-based FB electrolytes. We have also recently shown that solubility of zwitterionic triazine derivative was dramatically improved by increasing the supporting electrolyte concentration of KCl from 1 mol L^{-1} to 3 mol L^{-1}.[14]

Due to such remarkable advantages of using additives, in this work, we proposed to use 7-amino-4-hydroxy-2-napthalenesulfonic acid (**AHSQ**, Scheme 1) as a molecular spectator in **GAL**-KOH electrolytes. The former system was selected because it is an inexpensive precursor to prepare azo dyes of industrial applications and allows one to increase the concentration of positively charged counterions (e.g., Na^+, K^+, or Li^+ ions) in alkaline solutions; its substituent groups $-NH_2$, −OH, and $-SO_3H$ provide high solubility when undergoing acid−base neutralization reactions.[32−34] We demonstrated the feasibility of using this molecular spectator to significantly improve the solubility of the **GAL** electroactive material. The **GAL**−KOH−**AHSQ** FB electrolyte maintained good cycling stability when operating outside a glovebox.

2. RESULTS AND DISCUSSION

2.1. Cycling Stability under an Inert Atmosphere.

Encouraged by the advantages of storing two electrons per **GAL** molecule in alkaline aqueous FB negolytes, we examined the electrochemistry of this electrolyte in the presence of additive **AHSQ** with the aim to improve its volummetric capacity. The reversible reduction process of $\mathbf{GAL}_{ox}^{2-}$ to form $\mathbf{GAL}_{red}^{4-}$ species was reported be followed by ion pairing (with n number of cations $\mathbf{M}^+$, e.g., Na^+, K^+, and Li^+) and $\mathbf{H}^+$ transfer interactions:[1]

$$\mathbf{GAL}_{ox}^{2-} + 2e^- \rightleftharpoons \mathbf{GAL}_{red}^{4-} \qquad E^0,\ k_s \tag{1}$$

$$\mathbf{GAL}_{red}^{4-} + nM^+ \rightleftharpoons M_n\mathbf{GAL}_{red}^{n-4} \qquad K_{ion} = k_{f1}/k_{b1} \tag{2}$$

$$\mathbf{GAL}_{red}^{4-} + nH^+ \rightleftharpoons H_n\mathbf{GAL}_{red}^{n-4} \qquad K_{PT} = k_{f2}/k_{b2} \tag{3}$$

The solubility of **GAL** in this work was estimated to be 0.117 mol L^{-1} in 1 mol L^{-1} KOH at an approximate room temperature of 21 °C. However, it was not possible to test a flow cell with this electrolyte, because when oxygen was removed from the solution, partial precipitation of the material was observed. The addition of **AHSQ** (in proportions less than 1:3 of **GAL** and **AHSQ**, respectively) generated minimal effects on the cyclic voltammogram of the **GAL**−KOH electrolyte (Figure 1) and significantly improved the solubility of the electroactive material.

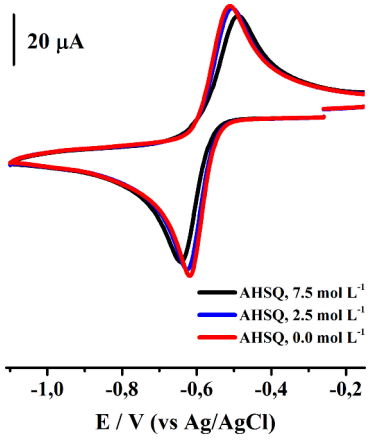

Figure 1. Cyclic voltammograms for the reduction process of 0.0025 mol L^{-1} **GAL** in 1 mol L^{-1} KOH, adding different concentrations of **AHSQ**. Scan rate of 0.1 V s^{-1}. WE: GC (d = 3 mm).

Considering a 1:1 ratio of species **GAL** and **AHSQ**, it was possible to prepare a negolyte solution having 0.2 mol L^{-1} **GAL** in 1 mol L^{-1} KOH. A flow cell was tested when 10 mL of the latter system was paired with a posolyte solution having excess KOH-sodium ferrocyanide. Both solutions were pumped through an in-house-made cell (composed of graphite and carbon felt electrodes) with flat flow fields and separated with a Nafion 212 cation-exchange membrane. The experimentation was carried out inside a nitrogen-filled glovebox by applying current densities of ±40 mA cm^{-2} during 75 cell cycles. The theoretical cell potential of the system **GAL**−KOH/$K_4Fe(CN)_6$ was reported to be 0.83 V.[1] When charging the cell, the **GAL** structures apparently undergoes reactions

https://doi.org/10.1021/acsaem.4c00971
ACS Appl. Energy Mater. XXXX, XXX, XXX−XXX

described by eqs 1−3, while one electron per electroactive molecule is withdraw from the KOH−ferrocyanide electrolyte. The cell started working as expected but suddenly lost all of its storage capacity after five cycles (Figure 2). At the end of the test, electroactive material was observed precipitating in the negolyte tank.

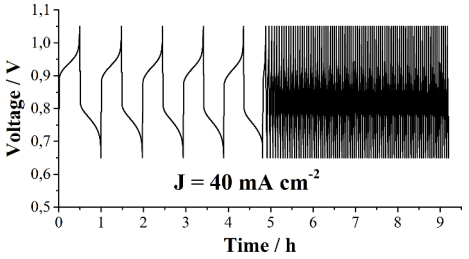

Figure 2. Galvanostatic cycling profile for 10 mL of 1.0 mol L^{-1} KOH solution containing 0.2 mol L^{-1} **GAL** and 0.2 mol L^{-1} **AHSQ**, using an excess KOH (40 mL) solution of potassium ferricyanide (0.035 mol L^{-1}) and sodium ferrocyanide (0.35 mol L^{-1}) as a posolyte and a cation-exchange membrane.

From Figure 2, it can be deduced that the cell stopped working before charging cycle 5. As reported by Martínez-González et al.,[1] the reduction process of **GAL** in NaOH occurs at a more positive potential value than in KOH, which means that **GAL** negatively charged species experience stronger and more directional interactions with Na^+ counterions than with K^+ species. Due to such strong stabilizing effect of Na^+ counterions on the negative charges of GAL_{ox}^{2-} structures, it is likely that the material precipitated once the Na^+ species contained in the sodium ferrocyanide solution passed across the cation-exchange membrane and interacted with $K_nGAL_{ox}^{n-2}$ complexes to form large precipitating aggregates $Na_nGAL_{ox}^{n-2}$. This assumption was reinforced by leaving a **GAL**-**AHSQ**-NaOH solution (of concentrations similar to those used in the cell test) inside the glovebox and detecting the insoluble material immediately. As this mechanistic pathway was not presented by Martínez-González et al., the following equation is added to describe those systems limited by ion-pairing interactions:

$$\mathbf{GAL}_{ox}^{2-} + nM^+ \rightarrow M_n\mathbf{GAL}_{ox}^{n-2}\ (\text{large precipitating aggregate}) \quad k_{f3} \qquad (4)$$

Note that, recently, the use of posolyte solutions having a mixure of Na^+ and K^+ ions has been proposed to improve the water solubility of ferrocyanide species.[11,35] As such counterions move freely across cation-exchange membranes, we suggest that, before opting for the latter solubilizing strategy, the degree of stability of the electroactive material in the negolyte tank be tested in the presence of both counterions. Otherwise, the experimental results may not be as expected. To avoid this problem, it was decided to analyze the system in the absence of Na^+ species.

For the next test, a 1:1.33 ratio of species **GAL** and **AHSQ** (respectively) was considered to prepare a negolyte solution having 0.15 mol L^{-1} **GAL** in 1 mol L^{-1} KOH. The flow cell was tested when pairing 8 mL of the latter system to a posolyte solution having excess KOH-potassium ferrocyanide and applying current densities of ±40 mA cm^{-2}. Seventy-five (75) charge−discharge cell cycles were carried out inside a nitrogen-filled glovebox, and the system exhibited good cycling stability, as detected from Figure 3.

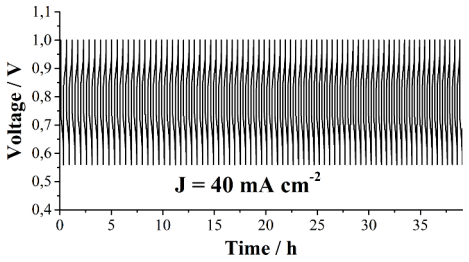

Figure 3. Galvanostatic cycling profile for 8 mL of 1.0 mol L^{-1} KOH solution containing 0.15 mol L^{-1} **GAL** and 0.2 mol L^{-1} **AHSQ**, using an excess KOH (35 mL) solution of potassium ferricyanide (0.035 mol L^{-1}) and ferrocyanide (0.35 mol L^{-1}) as a posolyte and a cation-exchange membrane.

When galvanostatically cycling the cell at 40 mA cm^{-2} (Figure 4A), Coulombic (CE > 99%) and round-trip energy (EE > 75%) efficiency values similar to those previously reported for the low concentration **GAL**-based electrolyte were obtained.[1]

As detected from Figure 4B, the cell operated with an initial volumetric capacity of 6.9 Ah L^{-1}, which is 85.8% of the theoretical capacity (8.04 Ah L^{-1}). These experimental values are higher than those reported by Martínez-González et al. (1.72 Ah L^{-1} and 64%) for a 0.05 mol L^{-1} **GAL**-KOH FB electrolyte. Therefore, the molecular spectator **AHSQ** worked successfully by improving the volumetric capacity of the **GAL**-KOH electrolyte. The low initial accessed capacity (64%) reported by Martínez-González et al., for the system operated outside the glovebox could be due to faradaic imbalance in the tanks caused by some traces of oxygen infiltration. The capacity of the **GAL**-**AHSQ**-KOH system (Figure 4B) tested here remains stable, gradually decreasing to ~6.0 Ah L^{-1} at the end of 75 cycles. In other words, the cell retained 87% of its initial operating capacity at the end of the experiment, projecting a capacity loss rate of 0.17% per cycle. Since no crossover of **GAL** products across Nafion 212 was demonstrated by Martínez-González et al., it is proposed that the capacity loss detected when operating **GAL**-based alkaline FBs is due to a decomposition mechanism of the electroactive material.

The decomposition mechanism could involve the formation of polymers and because this is a property exhibited by a wide variety of phenoxazine structures.[36] Given that GAL_{ox}^{2-} and GAL_{red}^{4-} species have several negative charges that could limit their interaction, it is likely that the decomposition mechanism also involves a decarboxylation pathway that causes the molecules to lose negative charge, increasing the probability of interaction of the molecules to form polymers. The decarboxylation process of **GAL** upon reduction was previously demonstrated and it is known to be favored when increasing the temperature.[37,38] Therefore, in future work, it will be interesting to study the long-term cycling stability of **GAL**-KOH electrolytes as a function of the temperature as well.

2.2. Cell Test of a GAL Improved Electrolyte. Motivated by the result presented above, we decided to explore the feasibility of using the additive under less-restricted atmosphere conditions. By switching to a 1:3 ratio of **GAL** and **AHSQ** species, respectively, we were able to prepare a KOH

https://doi.org/10.1021/acsaem.4c00971
ACS Appl. Energy Mater. XXXX, XXX, XXX−XXX

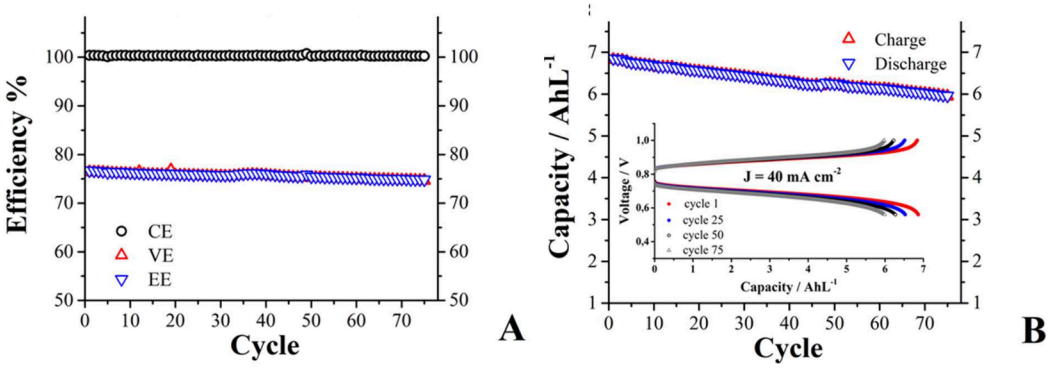

Figure 4. (A) Galvanostatic cycling efficiencies (Coulombic efficiency (CE), voltage efficiency (VE), and energy efficiency (EE)) for a flow cell of 0.83 V (as demonstrated by Martínez-González et al.[1]) composed of a **GAL**-KOH negolyte and a ferricyanide−ferrocyanide−KOH posolyte, operating at constant current density values of ±40 mA cm^{-2}. (B) Capacity retention as a function of cycle life, including a representation of the charge and discharge voltage profiles detected.

solution having 0.6 mol L^{-1} **GAL** compound (1.2 mol L^{-1} of electrons). Since this solution can store two electrons per electroactive molecule, it could operate as a negolyte with a theoretical capacity of 32 Ah L^{-1}, comparable to vanadium electrolyte.[10] However, it should be considered that the excessive use of additives could significantly compromise the kinetics of electroactive materials due to changes in the viscosity of the medium.

For example, using acetic acid as a cosolvent (H_2O + CH_3COOH volume ratio of 1:1), Li et al.[39] enhanced the solubility of the electroactive material Basic Blue 3 up to 2.5 mol L^{-1} in 3.5 mol L^{-1} H_2SO_4, demonstrating a high theoretical volumetric capacity of 134 Ah L^{-1} for the electrolyte. Despite this exceptional improvement in solubility, the authors reported a cell working with 0.05 mol L^{-1} of electroactive material, since the system exhibited kinetic complications, even at this low concentration of active material. In the system studied here, a large number of species K^+ are indirectly added to the solution when deprotonating each molecule of **GAL** and **AHSQ** by 3 and 2 equiv of KOH, respectively. In order to minimize the possibly negative effects of the counterions in excess and additive molecules on the electron transfer kinetics of the **GAL**-**AHSQ**-KOH system, for future work, it will be necessary to work on the optimization of its components.

To demonstrate the cycling stability of the improved **GAL**-**AHSQ**-KOH electrolyte in the presence of some traces of oxygen, we tested a FB cell outside the glovebox (passing nitrogen gas at the top of the tanks) putting 0.3 mol L^{-1} **GAL**, 0.45 mol L^{-1} **AHSQ** and 1 mol L^{-1} KOH in the negoltye tank. The electrolyte was characterized by cyclic voltammetry, and the obtained voltammogram is compared (Figure 5) to the one presented in Figure 1 for a low concentration of analyte. The cyclic voltammogram obtained from the solution tested as a FB negoltye (Figure 3) in the previous section is also presented.

The current intensity differences detected from the normalized voltammograms versus the analyte concentration C^* are related to changes in the solvation spheres of electroactive material due to increases in the concentration of **GAL**, **AHSQ** and K^+ species in the solution.[40−42] The ohmic drop resistance measured (using a conventional electrochemical cell) for the different electrolyte formulations did not change significantly and was within the range of 10−15 Ω. However, the peak-to-peak potential separation ($\Delta E_p = E_{pa} - E_{pc}$, where E_{pa} and E_{pc} are the oxidation and reduction peaks,

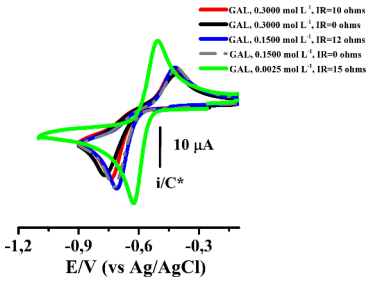

Figure 5. Cyclic voltammograms for the reduction process of **GAL** compound in 1 mol L^{-1} KOH, adding (green line) 0.0025 mol L^{-1}, (gray and blue lines) 0.2 mol L^{-1} and (black and red lines) 0.45 mol L^{-1} of **AHSQ** to the solution. C^* represents the concentration of the analyte. Scan rate of 0.1 V s^{-1}. WE: GC (d = 3 mm).

respectively) of the voltammogram changed from 124 mV to 300 mV when varying C^* from 0.0025 mol L^{-1} to 0.3 mol L^{-1}, which apparently reveals a slowdown in the kinetics of the reaction,[1,41,42] which could be due to an increase in the viscosity of the medium and the effects of the additive and counterions. Despite this apparent loss in reversibility, the FB cell exhibited good galvanostatic cycling stability upon applying 50 mA cm^{-2} (Figure 6). The Coulombic efficiency resulted to be >98%, while the energy efficiency started from 65% and stabilized at 58%. Such energy efficiency value is lower than the one reported by Martínez-González et al.,[1] and this is because the authors cycled their cell by applying a much lower current density (±5 mA cm^{-2} vs ±50 mA cm^{-2}).

During the first charge−discharge cell cycle, there was a significant amount of dissolved oxygen in the tanks, because the battery test began at the same time the nitrogen valve was opened. From the second cycle, the accessible initial capacity was 11.6 Ah L^{-1}, which is 72.1% of the theoretical capacity (16.06 Ah L^{-1}). 72.1% is a significantly higher value than the one reported by Martínez-González et al.,[1] (64%) for the **GAL**-KOH cell operated outside the glovebox with C^* = 0.05 mol L^{-1}. This could indicate that reactions between electrogenerated species and oxygen tend to become unfavorable as **GAL** concentration increases. The cell retained 88% of its initial operating capacity at the end of 110 charge−discharge cell cycles, projecting a capacity loss rate of 0.11% per cycle. Finally, the experimental volumetric capacity of the system studied here (11.6 Ah L^{-1}) is comparable to that of other reported aqueous organic FB negolytes. For instance,

https://doi.org/10.1021/acsaem.4c00971
ACS Appl. Energy Mater. XXXX, XXX, XXX−XXX

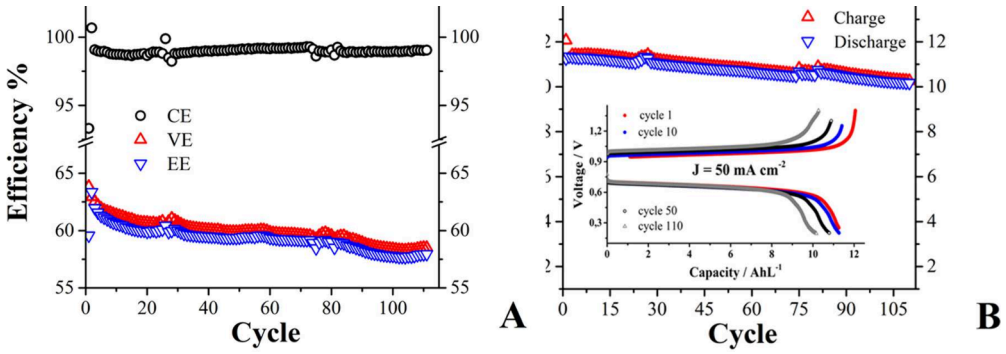

Figure 6. (A) Galvanostatic cycling efficiencies (CE, VE and EE, Coulombic efficiency (CE), voltage efficiency, (VE) and energy efficiency (EE)) for 9.5 mL of 1.0 mol L^{-1} KOH solution containing 0.3 mol L^{-1} **GAL** and 0.45 mol L^{-1} **AHSQ**, using an excess KOH (60 mL) solution of potassium ferricyanide (0.05 mol L^{-1}) and ferrocyanide (0.32 mol L^{-1}) as a posolyte and a cation-exchange membrane, applying constant current values of ±50 mA cm^{-2}. (B) Capacity retention as a function of cycle life, including a representation of the charge and discharge voltage profiles detected.

riboflavin-5-monophosphate sodium salt dissolved in 1.0 mol L^{-1} KOH + 3 mol L^{-1} nicotinamide exhibited an experimental capacity of 5.03 Ah L^{-1}.[43] An alizarin-based negolyte was also studied in KOH, reporting an experimental value of 6.1 Ah L^{-1}.[44] The corresponding values for methyl viologen-KCl, phenylene-bridged bispyridinium−KCl and DIQUAT−KCl solutions were reported to be 13.50 Ah L^{-1},[45] 20.00 Ah L^{-1},[46] and 4.18 Ah L^{-1},[47] respectively.

Next, to shed light on the reduction process of the improved electrolyte, the effect of each main component varied (protons, counterions, and additive) in the formulation were separately examined by cyclic voltammetry. The quasi-reversible voltammetric response (Figure 7A, red line) of 0.001 mol L^{-1} **GAL**

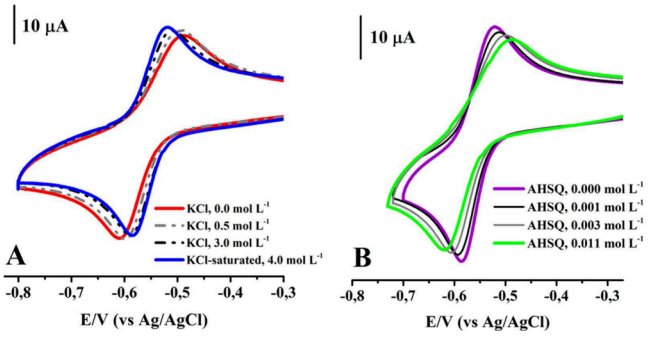

Figure 7. Cyclic voltammograms for the reduction process of 0.001 mol L^{-1} **GAL** in (A) 1 mol L^{-1} KOH and (B) 3 mol L^{-1} KOH, adding different concentrations of **AHSQ** and KCl. Scan rate of 0.1 V s^{-1}. WE: GC (d = 3 mm).

compound in 1 mol L^{-1} KOH was taken as a reference system. The addition of KCl (to intensify the effect of ion pairing interactions, Figure 7A, blue line) to the solution considerably shortened the ΔE_p distance in the wave, evidencing that, in the absence of excess salt (e.g., in 1 mol L^{-1} KOH solution), the protonation reaction is the rate-determining step. To test **AHSQ** effects, the **GAL** solution contained 3 mol L^{-1} KOH and the cyclic voltammogram exhibited better reversibility (small values of ΔE_p detected in comparison with 1 mol L^{-1} KOH; see Figure 7) since under this condition (3 mol L^{-1} KOH) the protonation reaction is not favored.

By adding few equivalents of **AHSQ** (Figure 7B) to the latter solution, an increase in peak-to-peak potential separation was detected, the oxidation signal broadened and the current intensity of both peaks decreased considerably, suggesting an interaction between GAL_{ox}^{2-} and **AHSQ** molecules. In other words, if the additive and GAL_{ox}^{2-} molecules interact before being reduced, larger species diffuse to the electrode, and this phenomenon decreases the diffusion coefficient. As a result, less current is expected in both peaks when **AHSQ** is added to the solution. This behavior is similar to the one reported for electrochemically controlled inclusion processes between host−guest molecules.[48]

Due to the interaction between GAL_{ox}^{2-} and **AHSQ**, it is likely that the additive behaves as a bulky substituent group that exerts steric hindrance to the functional groups because it also has negative charges; so the charge-transfer process is affected and becomes the rate-determining step, as exhibited by a large peak-to-peak separation in the response (Figure 7B, green line). So, the additive increases the volumetric capacity of the electrolyte, but there is a kinetics price to pay for this advantage. Without the additive, the negative charges of the **GAL** species tend to be neutralized to a certain degree by the positive charges of the species K^+ that are in excess in solution. Among the substituent groups that the additive has, the one containing an amino group could be via the interaction with GAL_{ox}^{2-} species, since this type of substituent group has been extensively used to modify the structure of other phenoxazine derivatives.[37,49]

In summary, an inexpensive molecular spectator (**AHSQ**) was introduced to increase the unexpectedly low solubility of **GAL** electroactive material in KOH. Although the additive slightly compromises the electron transfer kinetics of the FB electrolyte, it significantly improved its volumetric capacity. The cycling stability of the improved **GAL**-**AHSQ**-KOH negolyte solution was demonstrated by operating an FB cell outside a glovebox. This study opens the gap for searching **AHSQ** derivatives as molecular spectators to improve the volumetric capacity of other alkaline FB electrolytes. For future work, it will be important to study the decomposition mechanism of **GAL**-KOH electrolytes to work on its molecular design and/or on the selection of the appropriate additive that will allow improving the degree of stability of the electrogenerated **GAL** species in the presence of some traces of oxygen. Furthermore, and considering a reformulation of the electrolyte, it will be possible to use the maximum volumetric capacity (32 Ah L^{-1}) demonstrated in this work for a **GAL**-**AHSQ**-KOH negolyte.

https://doi.org/10.1021/acsaem.4c00971
ACS Appl. Energy Mater. XXXX, XXX, XXX−XXX

3. EXPERIMENTAL SECTION

3.1. Chemicals. Electrochemical experiments were carried out using **GAL**-KOH solutions in the absence and presence of different concentrations of molecular spectator 7-amino-4-hydroxy-2-napthalenesulfonic acid (**AHSQ**) and KCl. The chemicals were used as purchased. All of the solutions were maintained in an inert atmosphere by saturation with high-purity nitrogen at room temperature.

3.2. Cyclic Voltammetry Tests. The cyclic voltammograms were performed using a multichannel SP-240 potentiostat/galvanostat from Biologic (France) with EC-Lab software. The experiments were carried out applying 95% automatic IR drop compensation (Ru values ranging from 5 Ω to 15 Ω) evaluated with the ZIR tool. A GC disk electrode (d = 3 mm) was used as a working electrode; its surface was polished with 0.25 μm diamond powder (Büehler) and rinsed with distilled water. An aqueous reference electrode Ag/AgCl and a platinum wire were used as the reference and auxiliary electrodes, respectively.

3.3. Flow Cell Tests. An in-house-made cell (containing graphite and carbon cloth electrodes) composed of two solid end plates with push-to-connect fittings was used. A cation-exchange membrane (Nafion 212) was sandwiched between the latter two carbon pieces. Two carbon electronic collectors were placed between each carbon electrode and each solid end plate of the cell stack. The electrochemical system was operated in continuous flow, pumping (using a Masterflex L/S, Cole-Parmer peristaltic pump) the positively and negatively charged liquids through TBL-FEP Teflon tubings (Themoplastic Biologic) to store them in separate two external tanks identified as posolyte and negolyte liquids, respectively. Different formulations of **GAL**-**AHSQ**-KOH solutions were tested as negolytes in the presence of an excess concentration of potassium ferrocyanide in the posolyte tank. During the battery tests, high-purity nitrogen was recirculated in the upper part of both tanks. The flow cell was galvanostatically charged-discharged using a battery testing system (LANHE, Model G340A) at constant current density values of 40 and 50 mA cm^{-2}.

4. CONCLUSIONS

An inexpensive molecular spectator (**AHSQ**) was introduced to modulate the unexpectedly low solubility of the **GAL** electroactive material (with a two-electron storage capacity) in alkaline flow battery negolytes. The formulation allowed for the preparation of solutions with a theoretical volumetric capacity of 32.00 Ah L^{-1}.

The additive slightly compromises the electron transfer kinetics of the FB electrolyte, and the cycling stability of an improved **GAL** electrolyte was demonstrated by operating a FB cell outside the glovebox (bubbling N_2 at the top of the tanks). The cell exhibited a Coulombic efficiency close to 98% and began operating with 72.1% of its theoretical capacity (16.06 Ah L^{-1}), retaining 88% of it after 110 cell cycles.

This study opens the gap for searching **AHSQ** derivatives as molecular spectators to improve the volumetric capacity of another alkaline FB electrolytes. The results demonstrate that significant improvement of electrolyte performance can be obtained with suitable additives.

AUTHOR INFORMATION

Corresponding Authors

Eduardo Martínez-González − *Department of Mechanical and Materials Engineering, Research Group of Battery Materials and Technologies, University of Turku, Turku FI-20014, Finland;* orcid.org/0000-0003-4511-2244; Email: emagon@utu.fi

Pekka Peljo − *Department of Mechanical and Materials Engineering, Research Group of Battery Materials and Technologies, University of Turku, Turku FI-20014, Finland;* orcid.org/0000-0002-1229-2261; Email: pekka.peljo@utu.fi

Complete contact information is available at: https://pubs.acs.org/10.1021/acsaem.4c00971

Notes

The authors declare no competing financial interest.

ACKNOWLEDGMENTS

The authors gratefully acknowledges the Academy Research Fellow funding (Grant Nos. 315739, 343791, 320071 and 343794) and BioFlow project (Grant No. 343493) from Academy of Finland, and European Research Council through a Starting grant (Agreement No. 950038).

REFERENCES

(1) Martínez-González, E.; Amador-Bedolla, C.; Ugalde-Saldivar, V. M. Reversible Redox Chemistry in a Phenoxazine-Based Organic Compound: A Two-Electron Storage Negolyte for Alkaline Flow Batteries. *ACS Appl. Energy Mater.* **2022**, *5*, 14748−14759.

(2) Kwabi, D. G.; Ji, Y.; Aziz, M. J. Electrolyte lifetime in aqueous organic redox flow batteries: a critical review. *Chem. Rev.* **2020**, *120*, 6467−6489.

(3) Winsberg, J.; Hagemann, T.; Janoschka, T.; Hager, M. D.; Schubert, U. S. Redox-flow batteries: from metals to organic redox-active materials. *Angew. Chem., Int. Ed.* **2017**, *56*, 686−711.

(4) Zhao, Z.; Liu, X.; Zhang, M.; Zhang, L.; Zhang, C.; Li, X.; Yu, G. Development of flow battery technologies using the principles of sustainable chemistry. *Chem. Soc. Rev.* **2023**, *52*, 6031−6074.

(5) Yang, B.; Hoober-Burkhardt, L.; Wang, F.; Surya Prakash, G. K.; Narayanan, S. R. An inexpensive aqueous flow battery for large-scale electrical energy storage based on water-soluble organic redox couples. *J. Electrochem. Soc.* **2014**, *161*, A1371.

(6) Huskinson, B.; Marshak, M. P.; Suh, C.; Er, S.; Gerhardt, M. R.; Galvin, C. J.; Chen, X.; Aspuru-Guzik, A.; Gordon, R. G.; Aziz, M. J. A metal-free organic−inorganic aqueous flow battery. *Nature* **2014**, *505*, 195−198.

(7) Attanayake, N. H.; Kowalski, J. A.; Greco, K. V.; Casselman, M. D.; Milshtein, J. D.; Chapman, S. J.; Parkin, S. R.; Brushett, F. R.; Odom, S. A. Tailoring two-electron-donating phenothiazines to enable high-concentration redox electrolytes for use in nonaqueous redox flow batteries. *Chem. Mater.* **2019**, *31*, 4353−4363.

(8) Kwon, G.; Lee, S.; Hwang, J.; Shim, H.-S.; Lee, B.; Lee, M. H.; Ko, Y.; Jung, S.-K.; Ku, K.; Hong, J.; Kang, K. Multi-redox molecule for high-energy redox flow batteries. *Joule* **2018**, *2*, 1771−1782.

(9) Beh, E. S.; De Porcellinis, D.; Gracia, R. L.; Xia, K. T.; Gordon, R. G.; Aziz, M. J. A neutral pH aqueous organic−organometallic redox flow battery with extremely high capacity retention. *ACS Energy Lett.* **2017**, *2*, 639−644.

(10) Tang, G.; Yang, Z.; Xu, T. Two-electron storage electrolytes for aqueous organic redox flow batteries. *Cell Rep. Phys. Sci.* **2022**, *3*, 101195.

(11) Jin, S.; Jing, Y.; Kwabi, D. G.; Ji, Y.; Tong, L.; De Porcellinis, D.; Goulet, M.-A.; Pollack, D. A.; Gordon, R. G.; Aziz, M. J. A water-miscible quinone flow battery with high volumetric capacity and energy density. *ACS Energy Lett.* **2019**, *4*, 1342−1348.

(12) Lv, X.-L.; Sullivan, P.; Fu, H.-C.; Hu, X.; Liu, H.; Jin, S.; Li, W.; Feng, D. Dextrosil-viologen: a robust and sustainable anolyte for aqueous organic redox flow batteries. *ACS Energy Lett.* **2022**, *7*, 2428−2434.

(13) Pedraza, E.; de la Cruz, C.; Mavrandonakis, A.; Ventosa, E.; Rubio-Presa, R.; Sanz, R.; Senthilkumar, S. T.; Navalpotro, P.; Marcilla, R. Unprecedented Aqueous Solubility of TEMPO and its Application as High Capacity Catholyte for Aqueous Organic Redox Flow Batteries. *Adv. Energy Mater.* **2023**, *13*, 2301929.

(14) Asenjo-Pascual, J.; Wiberg, C.; Shahsavan, M.; Salmeron-Sanchez, I.; Mauleon, P.; Aviles Moreno, J. R.; Ocon, P.; Peljo, P. Sulfonate-Based Triazine Multiple-Electron Anolyte for Aqueous Organic Flow Batteries. *ACS Appl. Mater. Interfaces* **2023**, *15*, 36242−36249.
(15) Zhang, Y.; Li, F.; Li, T.; Zhang, M.; Yuan, Z.; Hou, G.; Fu, J.; Zhang, C.; Li, X. Insights into an air-stable methylene blue catholyte towards kW-scale practical aqueous organic flow batteries. *Energy Environ. Sci.* **2023**, *16*, 231−240.
(16) Zhang, M.; Li, T.; Liu, X.; Zhang, C.; Li, X. Molecular Revealing the High-stable Polycyclic Azine Derivatives for Long-Lifetime Aqueous Organic Flow Batteries. *Adv. Funct. Mater.* **2024**, *34*, 2312608.
(17) Rubio-Presa, R.; Lubián, L.; Borlaf, M.; Ventosa, E.; Sanz, R. Addressing Practical Use of Viologen-Derivatives in Redox Flow Batteries through Molecular Engineering. *ACS Mater. Lett.* **2023**, *5*, 798−802.
(18) Fang, X.; Zeng, L.; Li, Z.; Robertson, L. A.; Shkrob, I. A.; Zhang, L.; Wei, X. A cooperative degradation pathway for organic phenoxazine catholytes in aqueous redox flow batteries. *Next Energy* **2023**, *1*, 100008.
(19) Kong, T.; Liu, J.; Zhou, X.; Xu, J.; Xie, Y.; Chen, J.; Li, X.; Wang, Y. Stable operation of aqueous organic redox flow batteries in air atmosphere. *Angew. Chem., Int. Ed.* **2023**, *62*, No. e202214819.
(20) Otteny, F.; Perner, V.; Wassy, D.; Kolek, M.; Bieker, P.; Winter, M.; Esser, B. Poly (vinylphenoxazine) as fast-charging cathode material for organic batteries. *ACS Sustainable Chem. Eng.* **2020**, *8*, 238−247.
(21) Onoabedje, E. A.; Egu, S. A.; Ezeokonkwo, M. A.; Okoro, U. C. Highlights of molecular structures and applications of phenothiazine & phenoxazine polycycles. *J. Mol. Struct.* **2019**, *1175*, 956−962.
(22) Lee, K.; Serdiuk, I. E.; Kwon, G.; Min, D. J.; Kang, K.; Park, S. Y.; Kwon, J. E. Phenoxazine as a high-voltage p-type redox center for organic battery cathode materials: small structural reorganization for faster charging and narrow operating voltage. *Energy Environ. Sci.* **2020**, *13*, 4142−4156.
(23) González, E.; Hernández, L.; Muñoz, J. Á.; Blázquez, M. L.; Ballester, A.; González, F. Electron shuttles stimulate the reductive dissolution of jarosite by Acidiphilium cryptum. *Hydrometallurgy* **2020**, *194*, 105351.
(24) Mukerjee, P.; Ghosh, A. K. The effect of urea on methylene blue, its self-association, and interaction with polyelectrolytes in aqueous solution. *J. Phys. Chem.* **1963**, *67*, 193−197.
(25) Bourdon, R.; Peljo, P.; Méndez, M. A.; Olaya, A. J.; De Jonghe-Risse, J.; Vrubel, H.; Girault, H. H. Chaotropic agents boosting the performance of photoionic cells. *J. Phys. Chem. C* **2015**, *119*, 4728−4735.
(26) Moelbert, S.; Normand, B.; De Los Rios, P. Kosmotropes and chaotropes: modelling preferential exclusion, binding and aggregate stability. *Biophys. Chem.* **2004**, *112*, 45−57.
(27) Hamlin, J.; Phillips, D.; Whiting, A. UV/Visible spectroscopic studies of the effects of common salt and urea upon reactive dye solutions. *Dyes Pigm.* **1999**, *41*, 137−142.
(28) Reber, D.; Thurston, J. R.; Becker, M.; Pach, G. F.; Wagoner, M. E.; Robb, B. H.; Waters, S. E.; Marshak, M. P. Mediating anion-cation interactions to improve aqueous flow battery electrolytes. *Appl. Mater. Today* **2022**, *28*, 101512.
(29) Liu, L.; Yao, Y.; Wang, Z.; Lu, Y.-C. Viologen radical stabilization by molecular spectators for aqueous organic redox flow batteries. *Nano Energy* **2021**, *84*, 105897.
(30) Peng, K.; Li, Y.; Tang, G.; Liu, Y.; Yang, Z.; Xu, T. Solvation regulation to mitigate the decomposition of 2, 6-dihydroxyanthraquinone in aqueous organic redox flow batteries. *Energy Environ. Sci.* **2023**, *16*, 430−437.
(31) Lee, W.; Permatasari, A.; Kwon, B. W.; Kwon, Y. Performance evaluation of aqueous organic redox flow battery using anthraquinone-2, 7-disulfonic acid disodium salt and potassium iodide redox couple. *Chem. Eng. J.* **2019**, *358*, 1438−1445.
(32) Ionescu, M.; Mantsch, H. *Advances in Heterocyclic Chemistry*, Vol. *8*; Elsevier, 1967; pp 83−113.
(33) Thysiadis, S.; Katsamakas, S.; Mpousis, S.; Avramidis, N.; Efthimiopoulos, S.; Sarli, V. Design and synthesis of gallocyanine inhibitors of DKK1/LRP6 interactions for treatment of Alzheimer's disease. *Bioorg. Chem.* **2018**, *80*, 230−244.
(34) Doğan, F.; Kaya, I.; Temizkan, K. Multi-response behavior of aminosulfonaphthole system. *J. Mol. Catal. B: Enzym.* **2016**, *133*, 234−245.
(35) Jin, S.; Fell, E. M.; Vina-Lopez, L.; Jing, Y.; Michalak, P. W.; Gordon, R. G.; Aziz, M. J. Near neutral pH redox flow battery with low permeability and long-lifetime phosphonated viologen active species. *Adv. Energy Mater.* **2020**, *10*, 2000100.
(36) Schlereth, D. D.; Karyakin, A. A. Electropolymerization of phenothiazine, phenoxazine and phenazine derivatives: characterization of the polymers by UV-visible difference spectroelectrochemistry and Fourier transform IR spectroscopy. *J. Electroanal. Chem.* **1995**, *395*, 221−232.
(37) Hughes, N. *Rodd's Chemistry of Carbon Compounds*; Elsevier, 1964; pp 403−436.
(38) Kehrmann, F.; Beyer, A. Über die Methylierung des Gallocyanins, des Pyrogallins und des Azurins.(Vorläufige Mitteilung.). *Ber. Dtsch. Chem. Gesells.* **1912**, *45*, 3338−3345.
(39) Li, H.; Fan, H.; Ravivarma, M.; Hu, B.; Feng, Y.; Song, J. A stable organic dye catholyte for long-life aqueous flow batteries. *Chem. Commun.* **2020**, *56*, 13824−13827.
(40) Mahajan, R. K.; Chawla, J.; Bakshi, M. S. Effects of monomeric and polymeric glycol additives on micellar properties of Tween non-ionic surfactants as studied by cyclic voltammetry. *Colloids Surf., A* **2004**, *237*, 119−124.
(41) Bard, A. J.; Faulkner, L. R. *Electrochemical Methods: Fundamentals and Applications*, 2nd Edition; Wiley, 2001; pp 1−833.
(42) Savéant, J.-M. *Elements of Molecular and Biomolecular Electrochemistry: An Electrochemical Approach to Electron Transfer Chemistry*; John Wiley & Sons, 2006.
(43) Orita, A.; Verde, M. G.; Sakai, M.; Meng, Y. S. A biomimetic redox flow battery based on flavin mononucleotide. *Nat. Commun.* **2016**, *7*, 13230.
(44) Liu, Y.; Lu, S.; Chen, S.; Wang, H.; Zhang, J.; Xiang, Y. A sustainable redox flow battery with alizarin-based aqueous organic electrolyte. *ACS Appl. Energy Mater.* **2019**, *2*, 2469−2474.
(45) DeBruler, C.; Hu, B.; Moss, J.; Liu, X.; Luo, J.; Sun, Y.; Liu, T. L. Designer two-electron storage viologen anolyte materials for neutral aqueous organic redox flow batteries. *Chem* **2017**, *3*, 961−978.
(46) Hu, S.; Li, T.; Huang, M.; Huang, J.; Li, W.; Wang, L.; Chen, Z.; Fu, Z.; Li, X.; Liang, Z. Phenylene-bridged bispyridinium with high capacity and stability for aqueous flow batteries. *Adv. Mater.* **2021**, *33*, 2005839.
(47) Lv, Y.; Liu, Y.; Feng, T.; Zhang, J.; Lu, S.; Wang, H.; Xiang, Y. Structure reorganization-controlled electron transfer of bipyridine derivatives as organic redox couples. *J. Mater. Chem. A* **2019**, *7*, 27016−27022.
(48) Ceroni, P.; Credi, A.; Venturi, M. *Electrochemistry of Functional Supramolecular Systems*; John Wiley & Sons, 2010.
(49) Michaelis, L.; Eagle, H. Some redox indicators. *J. Biol. Chem.* **1930**, *87*, 713−727.

https://doi.org/10.1021/acsaem.4c00971
ACS Appl. Energy Mater. XXXX, XXX, XXX−XXX